Recovery of nuclear magnetization under extreme inhomogeneous broadening

J. R. Bodart, V. P. Bork, T. Cull, H. Ma, P. A. Fedders, D. J. Leopold, and R. E. Norberg
Department of Physics, Washington University, St. Louis, Missouri 63130
(Received 21 May 1996)

A quantitative model is presented for the transient recovery of nuclear magnetization under conditions where nuclear spin dipolar relaxation to dilute relaxation centers proceeds without the intermediary of nuclear spin diffusion. The model is developed for rigid arrays in three, two, and one dimensions. Comparison with experimental results yields measures of effective relaxation rates and relaxation center concentrations. [S0163-1829(96)00745-X]

I. INTRODUCTION

Nuclear spin lattice relaxation for fixed nuclear spins in nonmetallic solids often takes place via internuclear spin-diffusive transport of magnetization[1–6] to the vicinity of relaxation centers such as paramagnetic ions,[1,7] dangling bonds, or effectively dilute $J=1$ molecular hydrogen.[8,9] However the spin diffusion can be suppressed by strong inhomogeneous broadening (from quadrupolar[6,10,11] or from magnetic[12] interactions) or by magic angle spinning,[13] etc. Without spin diffusion, the nuclear relaxation may be dominated by the direct dipolar interaction between the fixed nuclear spins and the rapidly relaxing relaxation centers. Summation of this process over the nuclear spins gives rise to a generally non-exponential recovery of nuclear magnetization towards equilibrium. We present and demonstrate a model which efficiently describes the magnetization recovery for such fixed nuclear spins in solids of various dimensionalities.

II. THEORY

This paper considers the relaxation of nuclear spins directly to relaxation centers, without the intermediary of spin diffusion. This is appropriate in a number of different cases but especially when nuclear spin diffusion is suppressed by inhomogeneous broadening. Situations will be examined in which the angular-averaged nuclear relaxation rate for a nuclear spin at a distance r from the relaxation center can be written as

$$\frac{1}{T_1}=\alpha\left(\frac{a}{r}\right)^6. \tag{1}$$

Here α is the relaxation rate for nuclei adjacent to (a distance a from) the relaxation center. Two such processes will be considered in detail.

First we consider the relaxation of nuclear spins by paramagnetic ions. In this case the system includes a relaxation center described by spin S and gyromagnetic ratio γ_s as well as nuclei described by I and γ_n. Rapid spin-lattice relaxation of S produces relaxation of nearby I via the dipolar interaction terms $I_{j\pm}\ S_{kz}(t)$. Assuming a Markoff process with characteristic time τ for S, the nuclear relaxation rate at r and θ is given by

$$\frac{1}{T_1}=\frac{3}{2}\frac{\gamma_s^2\gamma_n^2\hbar^2}{r^6}S(S+1)\frac{2\tau}{1+\omega_n^2\tau^2}\sin^2\theta\cos^2\theta \tag{2}$$

so that

$$\alpha=\frac{1}{5}\gamma_s^2\gamma_n^2\hbar^2S(S+1)\frac{2\tau}{1+\omega^2\tau^2}\frac{1}{a^6} \tag{3}$$

is the relaxation rate for nuclei adjacent to the relaxation center.

We define an effective concentration c_r as the number of relaxation centers divided by the number of total lattice sites. Thus, on the average, nuclear spins within an outer radius r_c interact primarily with a relaxation center at the center of a region of radius r_c. The relationship between r_c and c_r depends on the dimensionality of the system and the lattice structure or number of lattice points per unit volume. In three dimensions

$$c_r=\left(\frac{3f}{4\pi}\right)\left(\frac{a}{r_c}\right)^3, \tag{4a}$$

while in two dimensions

$$c_r=\frac{f}{\pi}\left(\frac{a}{r_c}\right)^2 \tag{4b}$$

and in one dimension

$$c_r=\frac{f}{2}\left(\frac{a}{r_c}\right), \tag{4c}$$

where the region per atom is fa^d in d dimensions. For example, $f=1$ for a substitutional impurity in a simple cubic lattice of side a and $f=16/(3\sqrt{3})$ for a diamond lattice.

The second case considers the relaxation of a nuclear spin to a molecular relaxation center of the same element, in our measurements deuterium. Assume that ω_q, a typical quadrupole splitting, is much greater than the nuclear dipolar linewidth. In this case one obtains the formula[6]

$$\alpha\cong 2\left(\frac{\omega_d}{\omega_q}\right)^2\frac{1}{T_{2c}}, \tag{5}$$

where ω_d describes the dipolar interaction between the nuclear spin in question and an adjacent relaxation center and T_{2c} is the nuclear transverse relaxation time of the mo-

lecular relaxation center. Because of the rapid fall off of $1/r^6$, very few nuclear spins will experience a significant relaxation from more than one relaxation center.

A well-known crude model of the spatial distribution of magnetization recovery illustrates dimensionality related signatures. Assume that each nuclear spin sees only one relaxation center and that there is a uniform distribution of spins around a relaxation center. $M_z(t)$ then is proportional to the volume around a relaxation center within which $T_1(r) \leqslant t$. Thus

$$\frac{M_z(t)}{M_0} = \frac{4\pi}{3}(a/r_c)^3 \tag{6}$$

using Eq. (1) then yields

$$\frac{M_z(t)}{M_0} = \frac{4\pi}{3}(\alpha t)^{1/2} \tag{7}$$

and one anticipates a $\sqrt{t}$ evolution of M_z for a three-dimensional system. The exponent in Eq. (7) is the dimensionality divided by six, because of r^{-6} and so one expects $t^{1/3}$ for two dimensions and $t^{1/6}$ for one dimension.

A. Three-dimensional solids

Consider the spin-lattice recovery of nuclear magnetization for inhomogeneously broadened nuclear spins interacting with dilute relaxation centers separated by many internuclear near neighbor distances. Nuclei interacting with a single relaxation center contribute recovering magnetizations as the sum of exponential recoveries for the various spins I_j,

$$M_z(t) = \sum_j M_0(1 - e^{-t/T_{1j}}), \tag{8}$$

with T_{1j} given by Eq. (2) to be

$$T_{1j} = \alpha^{-1}(r_j/a)^6$$

and

$$M_z(t) = M_0 \sum_j (1 - e^{-\alpha t(a/r_j)^6}). \tag{9}$$

For a uniform distribution of spins, the magnetization can be written

$$M_z(t) = \frac{M_0}{V_0}\int_a^{r_c}[1 - e^{-\alpha t(a/r)^6}]d^3r, \tag{10}$$

where $V_0 = \int_a^{r_c} d^3r$ and

$$M_0 - M_z(t) = 4\pi\frac{M_0}{V_0}\int_a^{r_c} e^{-\alpha t(a/r)^6} r^2 dr. \tag{11}$$

We use the convenient but nonstandard definition of $c = (a/r_c)^d$ where d is the dimensionality of the system. Thus, from Eqs. (4), we obtain $c_r = (3f/4\pi)c$, $(f/\pi)c$, and $(f/2)c$ for $d = 3,2,1$. Thus, for example for Si, $(c_r/c) = 4(\pi\sqrt{3}) \cong 0.735$.

Using

$$u = \frac{a^3}{r^3}\sqrt{\alpha t} = c\sqrt{\alpha t}, \tag{12}$$

Eq. (11) becomes

$$\frac{M_0 - M_z(t)}{M_0} = \frac{1}{1-c}\int_{\sqrt{\alpha t}}^{\sqrt{c^2\alpha t}} \frac{e^{-u^2}}{u^2} du. \tag{13}$$

Integration by parts yields the recovery of nuclear longitudinal magnetization to be

$$\frac{M_0 - M_z(t)}{M_0} = \frac{1}{1-c}[F(c^2\alpha t) - cF(\alpha t)], \tag{14}$$

where

$$F(x) = e^{-x} - \sqrt{\pi x}\,\mathrm{erfc}\sqrt{x} \tag{15}$$

with the complementary error function

$$\mathrm{erfc}(z) = \frac{2}{\sqrt{\pi}}\int_z^\infty e^{-t^2} dt. \tag{16}$$

Equation (14) presents three interesting limiting cases for the recovering magnetization in a three-dimensional system.

(a) $\alpha t \ll 1$, $c^2\alpha t \ll 1$. For these short times Eq. (14) becomes

$$\frac{M_0 - M_z}{M_0} \simeq 1 - c\alpha t \tag{17}$$

and the $M_z(t)$ evolution begins proportional to t, with a characteristic time $(c\alpha)^{-1}$.

(b) $\alpha t \gg 1$, $c^2\alpha t \ll 1$. For these intermediate times

$$\frac{M_0 - M_z}{M_0} \simeq \frac{1}{1-c}(1 - \sqrt{\pi c^2 \alpha t}) \tag{18}$$

and the anticipated $\sqrt{t}$ regime emerges for M_z.

(c) $\alpha t \gg 1$, $c^2\alpha t \gg 1$. For these long times

$$\frac{M_0 - M_z}{M_0} \simeq \frac{e^{-c^2\alpha t}}{2c^2(1-c)\alpha t} \tag{19}$$

as M_0 is approached.

Figure 1 summarizes some aspects of the magnetization recoveries predicted by Eq. (14) for three-dimensional systems. Logarithmic presentations of M_z vs αt for six values of c show the dominance of $\sqrt{t}$ behavior over wide time intervals, especially for small c. At very short times M_z has the anticipated linear time dependence [Eq. (17)]

$$M_z(t) = M_0 \alpha c t. \tag{20}$$

For magnetization recovery in the three-dimensional case Eqs. (17), (18), and (19) provide some useful approximations. The intersection of extrapolated t and $\sqrt{t}$ fitted lines [Eqs. (17) and (18)] occurs at

$$\alpha t \simeq \pi, \tag{21}$$

where

$$M_z/M_0 \simeq c\pi. \tag{22}$$

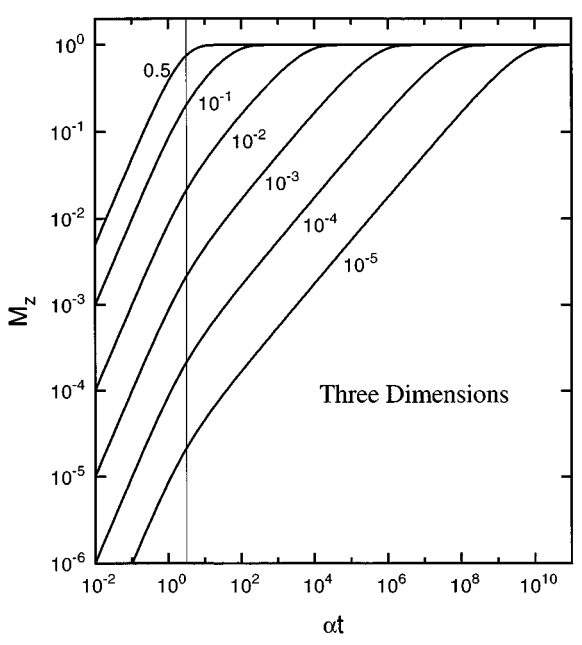

FIG. 1. Magnetization recoveries predicted for a three-dimensional array of spins and various relaxation center effective concentrations. The vertical line indicates $\alpha t=\pi$ and the transition from t to $t^{1/2}$, Eq. (21).

A vertical line in Fig. 1 indicates $\alpha t=\pi$.

Intersection of the fitted t behavior, Eq. (17), with $M_z=M_0$ occurs near

$$\alpha t \simeq c^{-1}. \tag{23}$$

The $\sqrt{t}$ fit of Eq. (18) extrapolates to intersect $M_z=M_0$ near

$$\alpha t \simeq (\pi c^2)^{-1}. \tag{24}$$

These approximations can be useful since, for small c, it may not be feasible to acquire reliable $M_z(t)$ data in the linear t regime, which requires $M_z/M_0 < c\pi$. Measurements restricted to larger M_z can only yield the bendover from $\sqrt{t}$ towards M_0 and a determination of the product $c^2\alpha$.

B. Two-dimensional solids

For a two-dimensional array of inhomogeneously broadened nuclear spins, a magnetization recovery analysis similar to that leading to Eq. (14) yields the result

$$\frac{M_0-M_z}{M_0}=\frac{c(\alpha t)^{1/3}}{3(1-c)}\left[\Gamma\left(-\frac{1}{3},c^3\alpha t\right)-\Gamma\left(-\frac{1}{3},\alpha t\right)\right], \tag{25}$$

where $\Gamma(-\frac{1}{3},x)$ is the incomplete γ function

$$\Gamma(a,x)=\int_x^\infty e^{-t}t^{a-1}dt. \tag{26}$$

This presents useful limiting cases for the two-dimensional case.

(a) $\alpha t \ll 1, c^3\alpha t \ll 1$. At very short times Eq. (25) becomes

$$\frac{M_0-M_z}{M_0}\simeq 1-\frac{c\alpha t}{2(1-c)}(1-c^3) \tag{27}$$

and again the $M_z(t)$ evolution begins proportional to t.

(b) $\alpha t \gg 1, c^3\alpha t \ll 1$. At intermediate times one finds

$$\frac{M_0-M_z}{M_0}\simeq\frac{1}{1-c}\left[1-c(\alpha t)^{1/3}\Gamma\left(\frac{2}{3}\right)\right] \tag{28}$$

with $\Gamma(\frac{2}{3})=1.354$ and the anticipated $t^{1/3}$ regime emerges.

(c) $\alpha t \gg 1, c^3\alpha t \gg 1$. At long times the approximate time evolution is

$$\frac{M_0-M_z}{M_0}\simeq\frac{e^{-c^3\alpha t}}{3(1-c)c^3\alpha t}. \tag{29}$$

Comparisons of Eqs. (27)–(29) yield useful approximations for the two-dimensional case. For small c, Eq. (27) becomes

$$M_z/M_0\simeq\frac{c\alpha t}{2}, \tag{30}$$

which intercepts $M_z=M_0$ at

$$c\alpha t\simeq 2. \tag{31}$$

For small c the intersection of the t and $t^{1/3}$ approximations, Eqs. (27) and (28), occurs at

$$\alpha t\simeq 4.46, \tag{32}$$

where the magnetization is

$$M_z/M_0\simeq 2.23c. \tag{33}$$

The $t^{1/3}$ approximation, Eq. (28), extrapolates to intersect M_0 at

$$c^3\alpha t\simeq 0.403. \tag{34}$$

Figure 2 shows magnetization recoveries predicted by Eq. (25) for two-dimensional systems. The conversion from linear t dependence to $t^{1/3}$ occurs near $\alpha t=4.46$, indicated in Fig. 2 by a vertical line.

C. One-dimensional solids

For a one-dimensional array of nuclear spins our model yields

$$\frac{M_0-M_z}{M_0}=\frac{c}{6(1-c)}(\alpha t)^{1/6}\times\left[\Gamma\left(-\frac{1}{6},c^6\alpha t\right)-\Gamma\left(-\frac{1}{6},\alpha t\right)\right]. \tag{35}$$

This presents the limiting cases.

(a) $\alpha t \ll 1, c^6\alpha t \ll 1$:

$$\frac{M_0-M_z}{M_0}\simeq 1-\frac{\alpha t c(1-c^6)}{5(1-c)} \tag{36}$$

and the early proportionality to t again appears in the one-dimensional case.

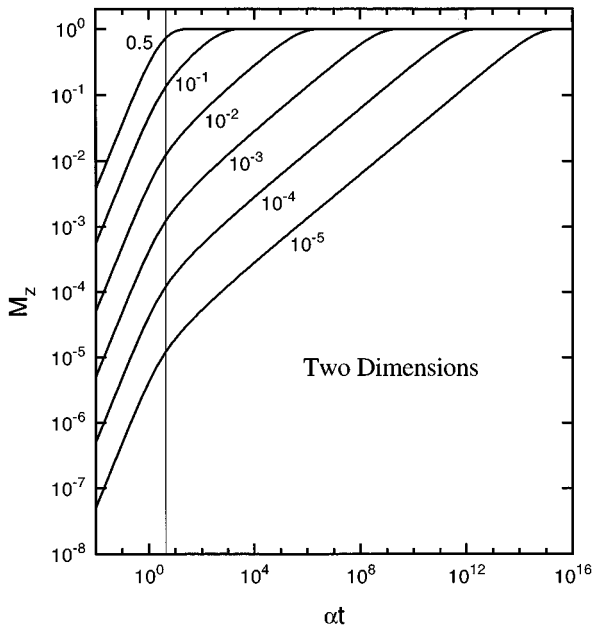

FIG. 2. Magnetization recoveries predicted for a two-dimensional array of spins and various relaxation center effective concentrations. The vertical line indicates $\alpha t = 4.46$ and the transition from t to $t^{1/3}$, Eq. (32).

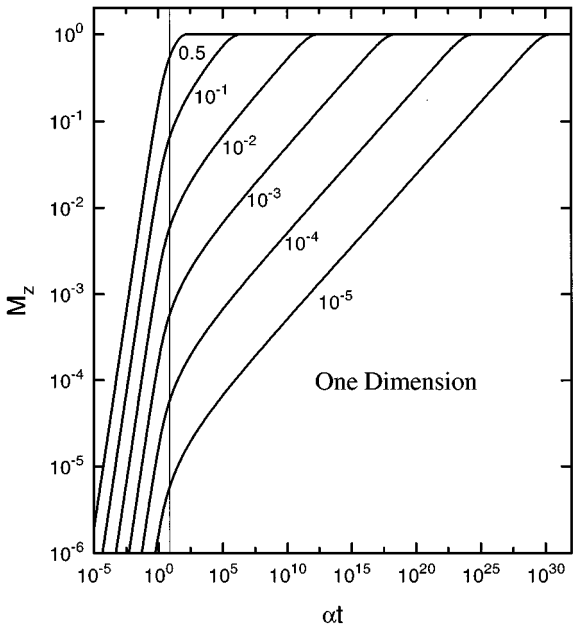

FIG. 3. Magnetization recoveries predicted for a one-dimensional array of spins and various relaxation center effective concentrations. The vertical line indicates $\alpha t = 7.75$ and the transition from t to $t^{1/6}$, Eq. (41).

(*b*) $\alpha t \gg 1, c^6 \alpha t \ll 1$:

$$\frac{M_0 - M_z}{M_0} \simeq \frac{1}{1-c}\left[1 - \frac{c(\alpha t)^{1/6}}{1-c}\Gamma\left(\frac{5}{6}\right)\right] \tag{37}$$

with $\Gamma(\frac{5}{6}) = 1.102$ and the anticipated $t^{1/6}$ regime appears.

(c) $\alpha t \gg 1, c^6 \alpha t \gg 1$:

$$\frac{M_0 - M_z}{M_0} \simeq \frac{e^{-c^6 \alpha t}}{6(1-c)c^6(\alpha t)}. \tag{38}$$

For magnetization recovery in the one-dimensional case Eqs. (36)–(38) can be compared, for small c. Equation (36) becomes

$$\frac{M_z}{M_0} \simeq \frac{c\alpha t}{5} \tag{39}$$

which extrapolates to M_0 at

$$c\alpha t \simeq 5. \tag{40}$$

The intersection of the t and $t^{1/6}$ approximations occurs near

$$\alpha t \simeq 7.75, \tag{41}$$

where the magnetization is

$$\frac{M_z}{M_0} \simeq 1.55c. \tag{42}$$

The $t^{1/6}$ approximation Eq. (38) intersects M_0 at

$$c^6 \alpha t \simeq 0.558. \tag{43}$$

Figure 3 shows magnetization recoveries predicted by Eq. (35) for one-dimensional systems. A vertical line indicates $\alpha t = 7.75$ and the conversion region from linear t dependence to $t^{1/6}$.

III. EXPERIMENTAL RESULTS

A. Deuterated amorphous germanium and silicon

Figure 4 shows a deuteron magnetization recovery over a range of 10^3 at 30 MHz and 81 K for a hydrogenated amor-

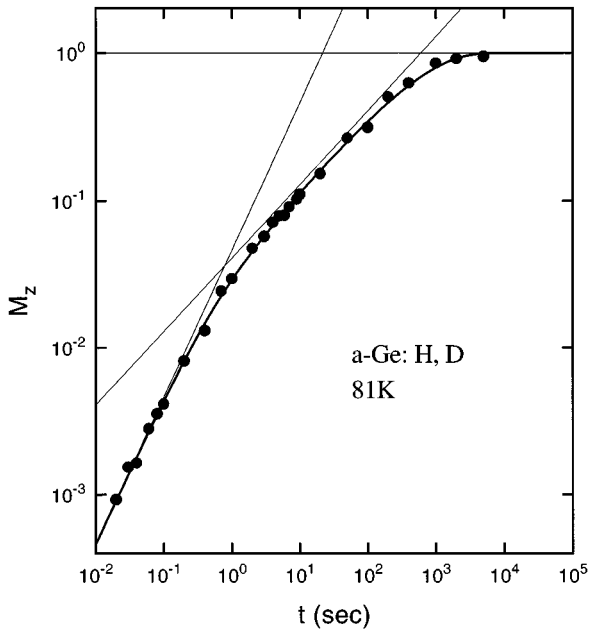

FIG. 4. Deuteron magnetization recovery for Ge-bonded D in *a*-Ge:H,D at 81 K. The heavy solid line shows the fit of the three-dimensional expression, Eq. (14).

phous germanium film (H686P) prepared by William Paul's group at Harvard University. The a-Ge:H,D film was plasma-deposited from GeH_4+D_2 onto a powered substrate at 150 °C. Analyses of deuteron and proton NMR spectra indicate that the film contains 17 at. % hydrogen, including 3.6 at. % H and 13.4 at. % D. Resolved deuteron NMR components include 9 at. % GeD, 0.97 at. % para-D_2 trapped on internal surfaces, and 2.6 at. % HD and D_2 with limited mobility in microvoids.

The deuteron magnetization component plotted in Fig. 4 is that of the axial symmetry 60 kHz quadrupolar doublet[14] arising from tightly bonded GeD. The data points are averages of $M_z(t)$ determined both from the quadrupolar doublet horns in $g(\omega)$ and from the corresponding 60 kHz beat on the $f(t)$ time transient spin echo. By averaging 40 960 data acquisitions for each magnetization recovery time, it has been possible to measure the Ge-bonded deuteron component magnetization down to $10^{-3}M_0$ and the data range includes all three anticipated regimes described by Fig. 1 and by Eqs. (17), (18), and (19). The curved line in Fig. 4 reflects an optimized fit of the full three-dimensional expression, Eq. (14), with parameters

$$M_0=1, \tag{44a}$$

$$\alpha=3.7\ \ \mathrm{sec}^{-1}, \tag{44b}$$

$$c=0.012. \tag{44c}$$

The sloping straight lines in Fig. 4 indicate the approximations of Eqs. (17) and (18) and make clear the t and $t^{1/2}$ data regimes and their intersections.

The anticipated rate parameter α depends on the nuclei and relaxation centers involved, on the lattice interval a, and on the dominant coupling mechanism for the transfer of nuclear magnetization.

For example, the relaxation rate α for a deuteron dipolar coupled to an adjacent relaxation center can be calculated via Eq. (3). For amorphous Si or Ge the separation is about $a=2.3\times10^{-8}$ cm. At this distance from a paramagnetic dangling bond defect with $s=1/2$ and the free electron gyromagnetic ratio γ_s, Eq. (3) yields

$$\alpha=5.9\times10^{12}J(\omega)\ \ \mathrm{sec}^{-1}. \tag{45}$$

Here the spectral density function

$$J(\omega)=\frac{2\omega_c}{\omega_c^2+\omega^2} \tag{46}$$

depends upon the electronic spin lattice relaxation rate $\omega_c=T_{1e}^{-1}$.

A reasonable value for T_{1e} is about 10^{-8} sec and corresponds via Eq. (3) to nuclear rates α near

$$\alpha=10^4\ \ \mathrm{sec}^{-1} \tag{47}$$

for adjacent deuterons at 30 MHz in a field of 4.7 T. The lack of agreement with the fitted $\alpha=3.7\ \mathrm{sec}^{-1}$, Eq. (44b), suggests that dangling bonds may not be the governing relaxation centers for the data of Fig. 4.

Furthermore in high quality hydrogenated amorphous silicon or germanium the density of paramagnetic dangling bonds is about $10^{16}\ \mathrm{cm}^{-3}$. For the a-Ge:H,D film H686P our ESR measurements yielded $N_\beta=2.8\times10^{16}\ \mathrm{cm}^{-3}$, or a fraction $c\simeq6\times10^{-7}$. The fitted deuteron magnetization recovery parameter $c=0.012\ \mathrm{cm}^{-3}$, Eq. (44c), is much too large to arise from paramagnetic dangling bonds.

Another possibility is that the relaxation of lattice-bonded deuterons in amorphous silicon and germanium films proceeds via internuclear dipolar interaction with rapidly relaxing molecular hydrogen relaxation centers, that is with effectively dilute[15] o-H_2 and/or p-D_2.

For a deuteron and an o-H_2 molecule at a 2.3×10^{-8} cm separation, Eq. (3) yields

$$\alpha=3.6\times10^7J(\omega). \tag{48}$$

For deuteron relaxation via an o-H_2 relaxation center the correlation frequency ω_c in Eq. (48) is the proton relaxation rate $1/T_1$ for effectively dilute o-H_2. For a field of 4.7 T the 81 K proton T_1 may be about 10^{-3} sec. Thus $\omega\gg\omega_c$, $J(\omega)\leqslant5\times10^{-14}$ sec, and

$$\alpha\leqslant1.8\times10^{-6}\ \ \mathrm{sec}^{-1}. \tag{49}$$

Therefore effectively dilute o-H_2 do not appear to be efficient relaxation centers for the (Fig. 4) magnetization of the lattice-bonded deuterons in the a-Ge film H686P.

A similar result would follow from a consideration of a deuteron dipolar T_1 process to effectively dilute p-D_2 molecules. However here there is another possibility. The lattice-bonded deuterons can transfer magnetization to the p-D_2 by means of the secular $\Delta M_J=0$ deuteron pair flip-flop dipolar T_2 process $I_{j\pm}S_{k\mp}$. In this case Eq. (5) applies and the limiting $J(\omega)$ is $2/\omega_c$ instead of $2\omega_c/\omega^2$ and for a D and p-D_2 at 2.3×10^{-8} cm separation the result is $\omega_c\simeq5600\ \mathrm{sec}^{-1}$. Equation (5) then yields

$$\alpha\simeq1\ \ \mathrm{sec}^{-1} \tag{50}$$

and the relaxation rate of lattice-bonded D to adjacent p-D_2 molecules can be many orders of magnitude larger than that to adjacent o-H_2. For the magnetization recovery data of Fig. 4 the fitted parameters $\alpha=3.7\ \mathrm{sec}^{-1}$ and $c=0.012$, Eqs. (44b) and (44c), are reasonable results if the relaxation centers are p-D_2 molecules. Our DMR line shape analyses for H686P have yielded a population of 0.97 at. % for the 76 kHz p-D_2 doublet component and a 2.6 at. % narrow central D_2 and HD microvoid population. The magnetization recovery fitted value $c=0.012$ [Eq. (44c)] is a reasonable concentration for p-D_2 relaxation centers.

Figure 5 shows $M_z(t)$ relaxation parameters αc and c fitted for the three-dimensional erfc expression, Eq. (14), to the recovery of the 66 kHz SiD deuteron quadrupolar doublet in a high quality mildly annealed (30 min. at 350 °C in helium atmosphere) a-Si:H,D film (XP2B) prepared at Xerox Palo Alto Research Center. At 14 temperatures between 11 and 300 K the relaxation rate αc varies by more than a factor of 40 and passes through a power law maximum near 60 K, with at T^{-2} variation on the high temperature side. Over the same temperature range the fitted concentration c remains nearly constant at 0.12, which probably reflects spin relax-

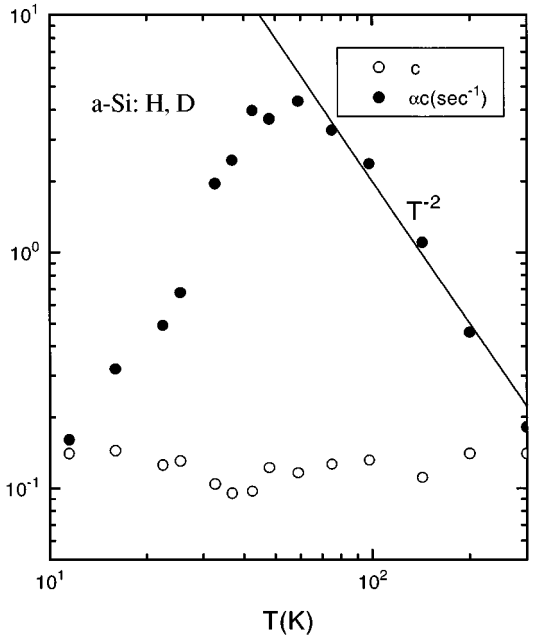

FIG. 5. Temperature variations of c and the rate αc for deuteron magnetization recoveries of Si-bonded D in a-Si:H,D.

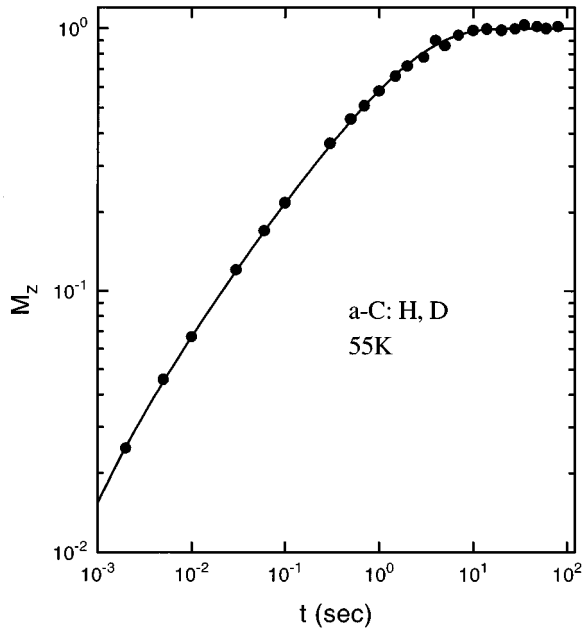

FIG. 6. Deuteron magnetization recovery for C-bonded D in a-C:H,D at 55 K. The solid line shows the fit of the three-dimensional expression, Eq. (14).

ation to para-D_2 relaxation centers. The c value, the αc range, and the T^{-2} dependence all support this interpretation.[8,9]

B. Deuterated amorphous carbon

The magnetization recovery of lattice-bonded D in amorphous carbon films is very different than that in amorphous silicon and germanium. For carbon the existence of both sp^2 and sp^3 binding prevents the inclusion of any appreciable population of molecular hydrogens and the relaxation of C-bonded D is governed by the presence of electronic paramagnetic defects.

Figure 6 shows the magnetization recovery of lattice-bonded deuterons at 55 K in a hydrogenated amorphous carbon film a-C:H,D No. 103 prepared in the laboratories of Bernard Feldman at the University of Missouri in St. Louis. The film was deposited from $C_3H_8+D_2$ onto an Al foil substrate and contained 21% D, 30% H, and 5% O. There is no evidence of appreciable molecular hydrogen or deuterium. Below 77 K the deuteron magnetic resonance spectrum consists of a 125 kHz quadrupolar doublet from C-bonded D. Figure 5 shows the recovery of the deuteron quadrupolar doublet at 55 K. The curved line shows the optimized fit of the three-dimensional recovery function given by Eq. (14) with fitting parameters

$$M_0 = 1, \tag{51a}$$

$$\alpha = 2.3\times 10^3 \ \ \mathrm{sec}^{-1}, \tag{51b}$$

$$c = 9.0\times 10^{-3}. \tag{51c}$$

Here the parameters α and c are in reasonable agreement with expectations for deuteron relaxation by electronic paramagnetic defects.

C. ^{29}Si in silicas

Devreux *et al.* have reported[13] measurements over a wide $M_z(t)$ range of the recovery of 71 MHz ^{29}Si magnetization in a series of silicas. Spin-diffusion among the spin 1/2 ^{29}Si was suppressed by magic angle spinning and the samples investigated included Cr^{3+}-doped crystalline and amorphous silica. Devreux kindly has provided us with their ^{29}Si $M_z(t)$ data tables and Fig. 7 shows an optimized fit of Eq. (13) to the ^{29}Si recovery in the amorphous silica. The erfc expression fits the data very well and the fitting parameters include

$$\alpha = 30.4 \ \ \mathrm{sec}^{-1}, \tag{52a}$$

$$c = 7.05\times 10^{-3}. \tag{52b}$$

For spin 1/2 ^{29}Si, spin 3/2 Cr^{3+}, and the separation a in silicas the anticipated rates α, Eq. (3), are somewhat larger than for electron dangling bonds, Eq. (46). The erfc fit, Eq. (52b), is an order of magnitude larger than the Cr concentration estimated[13] from preparation conditions for the amorphous silica.

Two of the silica samples reported were aerogels in which the majority of ^{29}Si reside in a nearly two-dimensional geometry. Figure 8 shows a fit of our two dimensional expression, Eq. (25), to the reported ^{29}Si magnetization recovery data for the Aerogel No. 1 sample. A substantial nearly $t^{1/3}$ regime is clear and the fitted two-dimensional recovery function shows an incipient bend over towards the linear t regime at the earliest data points reported. An optimized computer fit to the data yields fit parameters

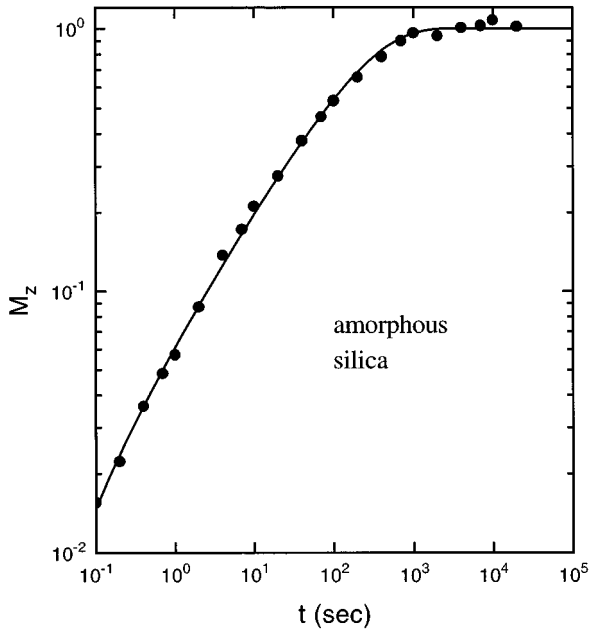

FIG. 7. ^{29}Si magnetization recovery under magic angle spinning in amorphous silica. The solid line shows the fit of the three dimensional expression Eq. (14). [Data provided by Devreux (Ref. 13).]

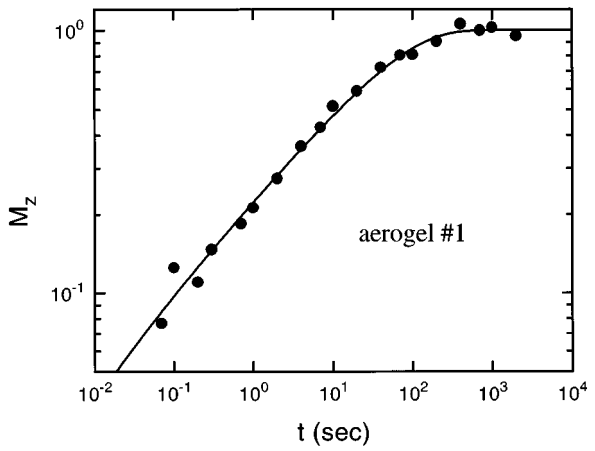

FIG. 8. ^{29}Si magnetization recovery for aerogel No. 1 under magic angle spinning. The solid line shows the fit of the two-dimensional expression Eq. (25). [Data provided by Devreux (Ref. 13)].

$$\alpha = 2440 \ \ \mathrm{sec}^{-1}, \tag{53a}$$

$$c = 1.3 \times 10^{-2}. \tag{53b}$$

Here again the fit parameters are consistent with relaxation to Cr^{3+} relaxation centers. The fitted c is 2.6 times larger than the Cr concentration estimated[13] from preparation conditions. The aerogel data of Fig. 8 are consistent with relaxation of an inhomogeneously broadened two-dimensional array of ^{29}Si.

Figures 7 and 8 have been plotted with the same ordinate and abscissa scale factors. The difference between the three dimensional Eq. (14) and two-dimensional Eq. (25) (predominantly $t^{1/2}$ and $t^{1/3}$) magnetization recoveries are evident for the two figures.

These aerogel data (Fig. 8) have been interpreted[13] in terms of a fractal noninteger dimensionality. Usually however fractal dimensionalities characterize paths in diffusion or atomic migration. For the recovery of magnetization of fixed nuclei only spatial separation is important and the significance of fractal dimensionality is not clear.

IV. CONCLUSIONS

The model presented provides a useful comprehensive description of the recovery of nuclear magnetization under extreme inhomogeneous broadening and in the presence of moderately dilute relaxation centers. If the concentration of relaxation centers is too small then NMR magnetization data, without some signal enhancement method, will be difficult to obtain in the initial linear M_z proportional to time regime, which requires measurements of $M_z \leqslant cM_0$. Without these early data three-dimensional magnetization recoveries only can determine the product $c^2\alpha$ and an independent determination of c by other means is required in order to determine the rates α. Nevertheless the relaxation model provides a practical vehicle for the quantitative determination of useful materials parameters for a wide range of samples. In cases where c can be determined from $M_z(t)$ (usually for $c > 10^{-3}$), the results are in reasonable agreement with concentrations otherwise determined for molecular hydrogen or for electronic relaxation centers.

The relaxation model has been shown to succeed for magnetization recoveries in three-dimensional and in two-dimensional arrays of nuclear spins. The one-dimensional expression should prove equally valid.

ACKNOWLEDGMENTS

This work has been supported in part by NSF DMR 93-05344 and by the Lillian Sirovich. Fund. Deuterated amorphous Si and Ge films were provided by the research groups directed by William Paul at Harvard and by Robert Street and James Boyce at Xerox PARC. Amorphous C films were provided by Bernard Feldman at the University of Missouri, St. Louis. We are grateful to Francois Devreux for providing ^{29}Si data reported[13] from the Ecole Polytechnique, Palaiseau.

[1] N. Bloembergen, Physica **15**, 386 (1949).
[2] P. G. de Gennes, J. Phys. Chem. Solids **7**, 345 (1958).
[3] W. E. Blumberg, Phys. Rev. **119**, 79 (1960).
[4] G. R. Khutsishvili, Sov. Phys. Usp. **8**, 743 (1966).
[5] I. J. Lowe and S. Gade, Phys. Rev. **156**, 817 (1967).
[6] P. A. Fedders, Phys. Rev. B **38**, 4740 (1988).
[7] H. E. Rorschack, Jr., Physica **30**, 38 (1964).
[8] M. S. Conradi and R. E. Norberg, Phys. Rev. B **24**, 2285 (1981).
[9] D. J. Leopold, J. B. Boyce, P. A. Fedders, and R. E. Norberg, Phys. Rev. B **26**, 6053 (1982).

[10] P. A. Fedders, Phys. Rev. B **33**, 5994 (1986).
[11] D. A. Jennings and W. H. Tantilla, J. Chem. Phys. **37**, 1874 (1962).
[12] C. E. Lee, I. Choi, J. E. Kim, and C. H. Lee, J. Phys. Soc. Jpn. **63**, 3509 (1994).
[13] F. Devreux, J. P. Boilot, F. Chaput, and B. Sapoval, Phys. Rev. Lett. **65**, 614 (1990).
[14] W. A. Turner, S. J. Jones, D. Pang, B. F. Bateman, J. H. Chen, Y. M. Li, F. C. Marques, A. E. Wetsel, P. Wickboldt, W. Paul, J. Bodart, R. E. Norberg, I. Elzawawi, and M. L. Theye, J. Appl. Phys. **67**, 7430 (1990).
[15] P. A. Fedders, R. Fisch, and R. E. Norberg, Phys. Rev. B **31**, 6887 (1985).